THE NEW CERN 50-MeV LINAC

E. Boltezar, H. Haseroth, W. Pirkl, G. Plass, T. Sherwood, U. Tallgren, P. Têtu, D. Warner, M. Weiss
CERN, Geneva, Switzerland

Summary

In this invited paper the new CERN 50-MeV linac will be described from several aspects including the general project background, a comparative treatment of services, components and phenomena along the beam, and some details of systems and techniques with emphasis on new approaches. A comprehensive list of references is included and a review of present status and performance.

Introduction

To introduce this general paper on the CERN 50-MeV linac we briefly enumerate the main sources of detailed information on the machine design. Starting with the general technical solutions proposed in the Project Study[1] (1973), several aspects of the machine design and parameters were updated and a status report[2] made at the 1976 Linac Conference, with full accounts of the RF structure design[3], the beam optics[4], the control system[5] and of measurement topics concerning the double drift harmonic buncher (DDHB)[6] and emittance[7]. At the 1979 US National Accelerator Conference (San Francisco), a summary of the linac design was presented with emphasis on experimental results at 0.75 MeV and 10 MeV, and on the first experience with 50-MeV operation for machine studies and then as the injector to the CERN accelerator complex[8].

In this conference many of the gaps can be filled, for example, by papers on the mechanical design[9], on the preinjector fast HT level control (bouncer)[10], the RF system[11] and the 50-MeV beam measurement system[12] with other papers on calibration[13], beam optics[14], HT formation[15] and a new ion source[16]. Many topics have also been treated in internal reports, often in more detail and appealing to a more specialized public.

Linacs used as injectors to large accelerator complexes must be conservatively designed and basically reliable, and these aspects do not normally lead to entirely novel solutions. In particular, at CERN the new linac was designed to replace the injector linac which had passed through several improvement programs since 1959, until its electrical and mechanical design and building limitations had been reached[17]. Nevertheless, if lacking in stability and peak current, this aging machine achieved less than 1% downtime in recent years; so the first aims for the new linac were to displace the intensity limitation to one of the subsequent synchrotrons[18] and yet keep comparable long-term reliability if possible in the changeover period as well. However there are features in the design of all systems which represent distinct advances in linac technology as will be detailed in the following sections.

The Project: History, Resources and Milestones

In May 1973, a study group was set up to make a project proposal concerning the upgrading or replacement of the 50-MeV linac injector to the CERN accelerator complex (booster synchrotron, the CERN 28-GeV PS and the Intersecting Storage Rings) which was in the process of being extended to 300 GeV by the SPS. The required improvement in intensity and quality (Table 1) was such that with experience gained on the 3-MeV experimental accelerator[19,20] on cavity calculations, low energy beam dynamics with space charge, measurements of high brilliance beams and on a thoroughly tested mechanical engineering approach, one already had the basis for an improved design. Accelerator design programs using linearized space charge forces for computing low energy beam transport (including bunching) and for defining focusing and matching in the linac proper were also available[21] and a double buncher scheme had been proposed[22]. In addition it had already been decided to develop a computer system based on PDP 11/45 computers for the linac, PS booster, and CERN PS combined control system. Thus the project proposal, presented and approved in October 1973[1], was in several important technical aspects more final and confident than one would expect after four months study (Table 2). By comparison, it was more difficult to arrive at the resources and time scale predictions.

Table 1. Beam Specification (Debunched)

Energy	50.0 MeV
Current	50 mA to 150 mA
Pulse duration	200
Repetition rate	2 pps
Normalised emittance	$<8\pi$ mm mrad (90% of beam)
Energy spread	±150 keV (90% of beam)

Table 2. Linac Parameters (as constructed)

Pre-accelerator	
Duoplasmatron ion source	I=300 mA
High gradient, two gap column	W=750 keV
750 keV (low energy) beam transport (LEBT)	
Transverse matching	18 quadrupoles (4 triplets)
Matching with bunchers	2 at 202.56 MHz
	1 at 405.12 MHz
Linear accelerator	
3 Alvarez tanks (202.56 MHz) with post couplers	
Focusing (FD) 131 quadrupoles (in drift-tubes)	
Synchronous Phase -35^{o} to -25^{o} (Tank 1) then -25^{o}	
50 MeV (High energy) Beam Transport (HEBT)	
Junction with existing line after 54 m (two bends)	
Transverse matching	14 quadrupoles
Debunchers	2 at 202.56 MHz, 1 at 405.12 MHz
Beam Measurements in 3 phase planes	

The net final result was that the linac was built and achieved its specified beam within its budget (23 MSF). The amount of mechanical engineering effort available, in particular at the start of the project was, however, not enough to keep within the original four-year schedule. From

another point of view, it is evident that the extra year for tests and the installation of ancillary apparatus contributed considerably to the very short delay between first acceleration to 50 MeV and reliable operation as an injector.

In Table 3 the final material costs are quoted by accelerator system while the in-house effort was 165 my. In Table 4, some key dates of the project realization are listed.

Table 3.

	MSFr.
Preaccelerator	2.0
LEBT	0.9
Structure	3.7
RF	2.6
Controls	3.7
HEBT	2.1
Bldg and Installations	5.0
Total material	20.0
Hired labor (about 65 my)	3.0
Total expenditure	23.0

This corresponds within a small margin to the original estimate of 21.3 MSFr. in 1973 prices, up-dated by the yearly index.

Table 4

Project approved	Oct. 73
Excavation started	Dec. 73
Preinj. + Controls area ready	Mar. 75
Building complete	Dec. 75
1st 750 keV beam	Dec. 75
LEBT	Dec. 76
Tank 1 ready	Apr. 77
1st 10 MeV beam	May 77
150 mA at 10 MeV	Sep. 77
Tank 3 ready	Mar. 78
Tank 2 ready	Aug. 78
1st 50 MeV beam	6 Sept 78
Design current (150 mA) attained	5 Oct. 78
1st test with booster	7 Oct. 78
Routine Operation	Dec. 78

An Overview of the Linac

Building and Machine Layout (Fig. 1)

The new linac was sited as closely as possible to the original linac within the limitations of existing buildings and the site topology. These limitations and the decision to separate the ancillary electronics, radio-frequency power sources and focusing power supplies from the accelerator led to a building section (Fig. 1) where accelerator tunnel, equipment room, and the air-conditioning plant are sited one on top of the other. To reduce tunnel costs the minimum acceptable cross-section was chosen; for an operating machine it is comfortably large but was very restricting vertically during installation. Other implications of the building position and design concerned the shape of the Faraday Cage and length of beam transfer lines (39 m longer than for old linac). The control room and its associated data room (housing the computers) were built in the corner of the existing South Hall.

Alignment Using External Reference Axes

The CERN PS orbit level, 433.66 m (above sea level) determines the linac beam axis height. A reference axis for preinjector, LEBT and accelerating cavities is parallel to but offset 0.6 m vertically and 0.3 m horizontally relative to the beam axis and is defined by four massive steel "monuments" situated near the two ends of the accelerating structure and the intertanks (Fig. 1).

Consider the low energy beam transport (LEBT Fig. 2) where each section is provided with a pair of targets and a (spirit) level reference face prealigned in the workshop to the physical or magnetic axis. With a microalignment telescope supported by a monument (on the offset axis) one can align elements to 0.15 mm (relatively) and 0.25 mm(absolutely) by adjustable tables to which the sections are bolted. Note that the last LEBT section is aligned to and supported from the first linac tank by a large diameter buncher (energy corrector, B3); similarly the first LEBT section and the preinjector column make one mechanical unit.

For the preinjector and linac tank alignment the same concept (as for the LEBT) is followed, i.e. easy adjustment and quick positional check. The relative alignments of tanks, girders and drift tubes are dealt with in other papers at this conference[9].

To be compatible with the PS injection and ejection lines the high energy beam transport (HEBT) elements use an alignment reference line 0.5 m vertically above the beam axis.

The Vacuum System

Throughout the linac, the vacuum system is based on turbomolecular pumping stations for initial pumping (or heavy gas load) with ion pumps for permanent high vacuum operation. Metal joints are used throughout with aluminium wire joints preferred in the LEBT and structure, diamond section aluminium joints in the HEBT. Clean assembly conditions consistent with the ion pumps and all-metal system were adopted with strict avoidance of organic matter in the preinjector and LEBT regions to minimize contamination of the high gradient HT column.

The particular pumping requirements of each region (defined by sector valves) are satisfied as follows:

a) for the preinjector two 1500 $1s^{-1}$ turbomolecular pumps cope with the continuous hydrogen load and achieve a pressure (one pump) of 5×10^{-5} Torr. The accelerating column and LEBT are connected only by the low conductance beam tube (20 $1s^{-1}$) through the "gun" assembly (Fig. 2). Further pumping at the entrance to the LEBT is provided by two 400 $1s^{-1}$ diode ion pumps.

b) The LEBT has a turbomolecular pumping station (450 $1s^{-1}$ turbopump and 10 $1s^{-1}$ backing pump) and a 400 $1s^{-1}$ triode ion pump for the DDHB region, supplemented recently by the 200 $1s^{-1}$ ion pump (Fig. 2). With ion pumps alone the operating pressure is $<1 \times 10^{-6}$ Torr.

c) For the accelerating structure, Fig. 3, there are two 450 ls^{-1} turbomolecular pumping stations per tank and one 1000 ls^{-1} triode ion pump per structure section (total 10). This allows rf conditioning with turbopumps alone and pump-down to 2×10^{-6}Torr in <2 hours after being at atmospheric pressure. Ultimate pressure is 2×10^{-7}Torr.

Focusing

Throughout the linac, quadrupoles of the BNL physical design[23] are used with some modifications in manufacturing techniques and different dimensions for LEBT singlets and triplet I.

Magnetic field tests were made on individual quadrupole magnets using a long coil field integration technique[24] to find the harmonic content of the field, the magnetic centre, the angular position of field symmetry planes relative to a keyway in the magnet yoke, and the important calibration for operation, $\int$(field gradient) dz as function of exciting current. To obtain precise results when iron proximity effects are important, measurements were made on realistic assemblies of two or three triplet elements. Each of the 125 drift tube quadrupoles was calibrated just before installation of the support girders in the cavities[13] to obtain absolute and comparative results, including effects of the copper drift tube shell and stainless steel bore tube. At normal operating fields the departure from linearity is >0.5% only for Types I, II and III (i.e. up to 5 MeV) while throughout the drift tube linac and within a quadrupole type, a constant relation gives sufficient accuracy to set the quadrupole field by the supply current.

The power supplies operate on the principle of a resonance circuit (LC) producing a half sine wave (2 ms long) which is clipped by a parallel transistor bank working in a feed-back circuit to give a precisely controlled flat top of >200μs with stability $\pm 2 \times 10^{-3}$during the pulse, and pulse-to pulse[25]. As the switching elements (thyristors) are rated at 1.0 kV, any increase in pulser current near this limit is made by increasing the capacitor bank (stored energy) and adjusting the triggering delay time.

With 160 quadrupole elements to power, the pulsers represent a considerable investment and control problem, so one connects magnets in series where possible within beam optics and pulser-load limitations. Thus, in the LEBT one has two pulsers per quadrupole triplet, in Tank I the first sixteen quadrupoles are powered individually, and where possible the others are in series pairs, while in the other tanks most quadrupoles are connected three to a pulser. The HEBT system (14 Type VII quadrupoles up to BH3) is not periodic so only one pairing was practical, and finally a total of 90 power supplies was required.

Bunching, Acceleration and Debunching.

Here we compare design, operation and associated hardware of the elements which affect the longitudinal motion. One has drift tube structures throughout and for the purposes of comparison the simple (non-relativistic) formula applies to the longitudinal action of any gap :

$$\Delta W = eV_{pk} T \cos\phi$$

with V_{pk} the peak voltage on a gap, W the kinetic energy, ϕ the RF phase of proton arrival (relative to positive maximum) and T the transit time factor , which is a function of gap geometry and energy.

For acceleration one generally has $\cos\phi$=0.80 to 0.90 whereas bunchers and debunchers normally give no net energy gain to the mean proton of a bunch i.e. $\cos\phi$=0. Radial defocusing is also important both at low energies and for bunchers, but its reduction with grids was not considered justifiable.

Structure Design. For each rf structure one aims to minimize the power for the required $\Delta W_{eff} = eV_{pk} T$, but with heavy beam loading, transient level and phase problems, severe aperture requirements, need to house focusing elements and need to maintain mechanical simplicity, the final solutions are inevitably compromises. The cavity dimensions, losses and dynamics coefficients (e.g. T) were computed using the program CLASL[26] for the three bunchers and the linac (128 unit cells). Generally, to ease fabrication and surface finish problems, we could accept 25% more rf power losses than for perfect copper (representing <10% of total power including beam loading).

The bunchers have moderate requirements in ΔW_{eff} (<35 keV) so the mechanical and dynamics contraints strongly influence the design. For the 202.56 MHz bunchers the chosen asymmetric design (half a unit cell) has a gap of 13 mm, aperture diameters 20 mm and 25 mm (for B1 and B3 respectively) giving acceptable values of T (0.71, 0.60). The half drift tube can house a quadrupole or beam transformer (d=180 mm) and the cavity diameter (700 mm) leads to an efficient rf design within mechanical constraints of incorporation in the Tank I input cover (B3). For the 405.12 MHz case (B2) the symmetric design gives the specified separation between the double drift harmonic buncher (DDHB) gaps. The beam dictated an aperture diameter of 18 mm (gap=10 mm) which gives T=0.36; the variation in T with radius across a well adjusted proton beam could help longitudinal matching[27]. To first order, the energy modulation of an unbunched beam (in DDHB) causes no real or reactive beam loading. All bunchers were made from mild steel, copper-plated to 15 μ, with aluminum wire joints for vacuum and rf contact.

The 202.56 MHz accelerating cavity geometries are dictated by the size of drift tubes (containing quadrupoles), need to maintain $0.2 < g/L < 0.35$ (high value of T), acceptable shunt impedance and the computed dynamics, which determines individual cell lengths[3]. The tank (cavity) lengths are mainly determined by the rf amplifier arrangement (one amplifier and feed loop for 10 MeV acceleration). The cavity diameters 0.94 m, 0.90 m, and 0.86 m, respectively, keep T high and rf losses near their minimum. Further design details are given elsewhere[9] (also under Accelerating Structure).

For the debunchers, the peak energy changes of ∿400 keV at 202.56 MHz make a high shunt impedance desirable. The large beam apertures cause

problems due to reduction of T and penetration of the electric field into the beam tube especially at 405.12 MHz (DB14).

Field Calibration. Several methods are available:
a) Effective field as a function of input power comes from cavity calculations (normalized by measured Q).
b) Field on the axis (hence T and tilt) by perturbation methods[13].
c) Observations on longitudinal dynamics at nominal rf level and comparison with computed predictions[13].

With methods a) and c) the cavity field is measured by the monitoring loops which couple to H_ϕ at the cavity wall.

For adjustment of buncher rf levels method a) is sufficient but b) has been used to confirm symmetry of field in the asymetric bunchers while c) has been applied to the DDHB using a fast probe[6] and also by reference to the 10 MeV beam characteristics. For debunchers c) is applicable in the longitudinal measurement line (DB12) by beam energy change versus phase shift.

Multipactoring. This problem in the initial powering of all rf cavities is discussed here by reference to the linac cavities. Ideally one needs a clean vacuum ($<10^{-5}$ Torr), temperature control of cavities, correct input match, variable feeder line length and control of the rf pulse rise time. Even so ionization pumps and ionization gauges directly on the tanks had to be switched off to obtain the initial erratic acceptance of power with a glow discharge (observed near the feed loops) and much evolution of gas from copper surfaces. After some hours (<12 hours) of steady improvement, power was eventually accepted up to 20% above nominal level on all pulses with ion pumps on, quadrupoles pulsing and rf amplifiers on slowest rise time. This process only takes a significant time when first powering a cavity.

In the single-gap cavities, the conditioning was sometimes lengthy with more apparent dependence on surface cleanliness and on relative timing of adjacent cavities (supposedly producing ions or electrons). However, during scheduled operation, the number of bad pulses one ascribes to multipactoring is negligible.

Evolution of the Beam along the Linac

To complement the two comprehensive approaches to beam optics[4,14], this section describes the beam qualitatively as it passes from preinjector to booster input. In Fig. 5 we give in one transverse plane and in the longitudinal plane, beam envelopes (2 x rms size in mm and in deg.) assuming computed results (modified by measurements where possible) with time (ns) as abscissa. The virtual longitudinal aperture is half the estimated bucket width. Note that the rms envelope representation is relevant for beam transport with space charge but it can seriously underestimate the beam limits if there are long tails on the density distributions.

Generally, this plot brings out the similarities between LEBT and HEBT, both transversely (envelopes and lens separations), and longitudinally, (transition from continuous to bunched beam and vice-versa). The preinjector which represents only 20 ns of acceleration at 6 MeV m^{-1} is designed to take the dense beam rapidly through a difficult space charge region. In the first part of the LEBT, an essentially round unbunched beam is contained by 4 quadrupole triplets, limited proportionally in diameter and angle (apertures AP1 and AP2) and steered (ST1 to ST4) to the DDHB. The bunching system performs a six-dimensional matching to the linac input with 6 quadrupoles and 3 bunchers compressing 80% of the beam into an ellipsoid of mean diameter 7 mm and length 10 mm. In the linac the +- focusing system starting with $\mu=30^o$ maintains a very small beam size, even with transverse emittance growth of 2.3 due to the compensatory reduction in the space charge effect and resulting increase of μ, an effect enhanced also by the growth in longitudinal emittance (x 5 measured). In HEBT there is rapid transverse growth to match the longer period of the focusing, while longitudinally, both energy spread and space charge act to increase the bunch length. Other features of the HEBT are an achromatic section between BH2 and BH3, and the use of debunchers to shape the energy spectrum.

Users Facilities on the Control System

Users have access over two maxiconsoles, two midiconsoles and two analog consoles in the control room, plus one mobile midiconsole in the equipment gallery. The midiconsoles each have four "knobs", one "access" card reader, a numeric keyboard, a touch panel for parameter and task selections and a color TV monitor. The latter displays any four beam transformers plus any four parameters (Fig. 6), where, given access, the operator can act, either by a "knob" or by the numeric keyboard. Synoptic displays are used for groups of parameters, e.g. the LEBT (Fig. 7) or the vacuum system (Fig. 8) where a valve or pump can be selected via the touch panel and acted on, registering as a visible status change on the display. The maxiconsole has additional facilities: a 611* storage scope, a video terminal, and a touch panel for measurement tasks. The analog console allows one to select and "hook" a parameter to any of four traces on two scopes or to a waveform digitizer which can "freeze" or, if necessary, store the display.

A powerful feature is the List Processor which takes any parameter name list and sends a matching list of values from a disk file, e.g. for setting tank quadrupoles. Value files can be prepared for different conditions, and later be activated by a touch panel or by a surveyor task.

One can, using only parameter names, write application programs in BASIC-11, FORTRAN 4+ or PASCAL, e.g. CORLIN (in BASIC), corrects the offset between desired and actual currents from the quadrupole pulsers, whereas TRACE, (in FORTRAN) predicts, from user input values, LEBT beam envelopes and emittances on the 611 storage scope. BASIC has also been convenient for log programs and ad-hoc programs where on-line debugging is essential[28].

*Tektronix

Particular Design Features

Preinjector

HT Equipment. The high-voltage generator (Cockcroft-Walton) and associated electronics, electronics platform and the original beam-loading compensation were bought from Haefely, Basle. For maintenance reasons an open Cockcroft-Walton was chosen. It operates at 5 kHz with maximum output 850 kV and 4 mA DC and is connected to the electronics platform by a 5-MΩ damping resistor. A three-stage isolation transformer rated at 7 kVA (14 kVA at reduced voltage) supplies power to the electronics platform. The insulation is rated at 300 kV per stage with 2500-MΩ resistors incorporated to ensure equal potential distribution. The original beam-loading compensation (bouncer), a compact two-tube arrangement housed in an oil-filled tank, has been replaced for maintenance and reliability reasons by an open (air-insulated) structure. This new bouncer uses only one tube, has a wider band width and shows better reliability than the previous system[10].

Ion Source. The original duo-plasmatron ion source of the old linac[29] was already modified some years ago[17]. For the reduced diameter of the accelerating column anode in the new linac, this source had to be made smaller, mainly by cutting away superfluous parts and redesigning the magnet coil, with most of the inner parts inter-changeable with the old source. Armco iron parts are nickel-plated, to provide corrosion protection. Another improvement was the replacement of the old oil-cooling system by a circuit using distilled water with 30% ethanol as corrosion inhibitor with a fluid-to-air heat exchanger on the electronics platform. The oil was a potentially serious hydrocarbon contamination risk for the column and the oxide cathode during source changes, compared to the relatively volatile water-ethanol mixture. In addition, one has less flow and circuit pressure for equivalent cooling.

The arc pulser consists of a delay line (defining the maximum pulse length) with a large series resistance to supply constant current to the source. Pulse length reduction is achieved by thyristors short-circuiting the arc when triggered.

Accelerating Column. The 750 kV accelerating column (built by HVEC) is a modified version of the CERN 500 kV design[30] with 19 sections (instead of 14), of the same diameter, which necessitated a reduction in anode and source diameters and larger radii on the central inner shielding rings. Both gap and gradient have increased from 43 kV cm^{-1} across 11.7 cm to 58 kV cm^{-1} across 12.9 cm and there is an intermediate electrode (as in the old linac) to improve voltage holding and focusing. The total capacity associated with the column is 2.6 nF of which 1.5 nF is connected via a 2 kΩ damping resistor to the bouncer. The dissipation of the stored energy (during column breakdown) has not caused observable damage. The cathode requires -4-kV bias to avoid frequent breakdown and high radiation levels, although this potential only forms a barrier against back-streaming electrons at the edge of the cathode hole.

The column is a structure made of ceramic rings glued together with epoxy resin and supported like a cantilever at the cathode end. With the column fully loaded and not under vacuum, the epoxy resin bond has a safety factor of 20 proved both by tests and by calculations (epoxy resin tensile strength ∿ 10N/mm^2). Nevertheless, for safety reasons, at the anode end a force is added (rope and counterweight) minimizing the bending moment along the column. Inside the cathode is the "gun", a tubular vacuum-tight structure containing the first magnetic triplet (T1), beam transformer (IM2), steering magnets ST1) and an electron trap. This assembly is bolted onto the column making one mechanical unit for support, alignment and vacuum (see Fig. 2).

Performance. The source geometry was optimized experimentally by adjusting its longitudinal position and the expansion-cup shape, but the required small Gaussian-type emittances seemed unavoidably associated with rather noisy pulse shapes at normal operating beam currents > 250 mA (and vice versa). One initially adjusts the operating parameters such as hydrogen flow, arc current and cathode current by reference to output current, pulse shape and emittance (measured at EM2). Measurements made over several months show that beam characteristics are stable and can be set to values stored in the control computer. Source lifetime, determined by cathode emission and anode erosion, is > 1 year in normal operation.

After a source change the conditioning of the evacuated column to 750 kV takes ∿ 1 hour when done automatically[15]. In typical operation the HT breakdown rate is ∿ 1/day. As this sometimes disturbs the source-computer interface, the source parameters are reset automatically.

LEBT

The LEBT has been designed to transport the preinjector beam, to shape it and to match it in both transverse and longitudinal planes (6 dimensions) to the linac input. Functionally it consists of a long unbunched beam section which provides an essentially round beam about 10 mm diameter at DDHB, and a bunching section which performs the matching to the linac via six quadrupoles and three bunchers.

Mechanical Engineering and Components. The main objectives in the mechanical concept of the LEBT were an easy and rapid alignment without disturbing the vacuum, a clean vacuum and the possibility to put diagnostic equipment in any of several foreseen places.

The part of the LEBT installed in the column cathode has been described above. Between the column output and DDHB, the LEBT is a classical beam line with five independent units mounted on individual supports and connected by flexible vacuum chambers. The bunching section, the last and most important part of the LEBT, is extremely crowded and forms one mechanical unit for alignment and support via its main element, a large diameter buncher (B3) which is bolted on and aligned to the first linac tank (see Fig. 2).

The diagnostic equipment, defining apertures (AP1, AP2) and beam stoppers use tantalum plates

which have a good resistance to beam damage. Nevertheless under certain focusing conditions the proton beam could eventually burn a hole through the stopper which forms part of the radiation safety interlock chain. Thus the stoppers have a safety device, an additional plate, which, if pierced by the beam develops an air leak and switches off the linac. More details of vacuum and alignment are given under corresponding headings.

Beam Optics[27]. The figure of merit for the LEBT/Linac beam optics is the measured (as previously computed) trapping efficiency of 80% which allows the design beam current at 50 MeV, 150 mA, to be obtained with < 200 mA injected into the linac (∿ 250 mA from the source). The position of bunchers was studied for beam currents between 50 and 250 mA and the optimum distances for trapping efficiency, bunching voltages and acceptable geometry determined. The distances from B1(202.56 MHz), B2 (405.12 MHz) and B3 (202.56 MHz) to the first linac gap are 101 cm, 86 cm and 16 cm, respectively (see Fig. 2). Note that for the highest currents the computed trapping remains > 80% in spite of severe linac input conditions (e.g., mean beam diameter ≈ 7 mm), which would allow us to provide more output current if necessary. In the bunching region one has sufficient quadrupoles to keep the beam well inside the 45 mm diameter aperture and to match it to the linac input.

Practical Aspects of Beam Matching. One needs a round axial beam at the input of the DDHB, < 10 mm diameter, limited proportionally in angle and diameter so as to have equal vertical and horizontal emittances. Thus one has to adjust the four triplets, the steering magnets (ST1 to ST4) and the apertures (AP1 and AP2) with reference to beam currents (IM3, IM4 and IM5) and emittance measurements at EM2 and EM3 (Fig. 2). On-line computer programs are available to derive quadrupole settings using the measured rms values as input data and steering settings, using mean beam positions. This procedure is even more necessary for adjustment of the bunching region quadrupoles to match to the linac acceptance. As noted above (bunching, field calibration) buncher amplitudes are set to computed values. Solutions for several beam conditions can be stored on the linac computer and parameters set by pressing one or more touch buttons.

Operation and Performance. An important aspect of the LEBT operation is the reproducibility and no further fine adjustment of parameters is required after setting-up. There is good transmission through the LEBT as an unlimited beam has decreased by only 15% (probably heavier particles) at the DDHB and there are no further losses to the linac input. The performance of the LEBT has fulfilled its design predictions in handling all beam conditions without reaching limitations in element position or strength. No down-time has yet been ascribed to LEBT malfunction.

Accelerating Structure

Many of the construction techniques first tried at CERN on the 3 MeV accelerator[19,20] were suitable for the 50 MeV accelerator structure[9] e.g., copper-clad steel fabrication, aluminium wire joints for rf and vacuum, and demountable drift tube support girders. The rf and beam duty cycle are < 10^{-3} and as the proton beam takes ∿ 70% of the RF power there is less reason for fanatical attention to cavity losses. All components except bulk tuner are demountable from outside the cavity while the intertanks are combined with end half cells into a demountable unit and the three tanks form a single vacuum system (Fig. 3). Before installing the girders in the cavity one has complete accessibility for mounting the drift tubes and for adjusting their relative alignment.

Cavities. The accelerating structure (Fig. 3) is divided into three tanks accelerating from 0.75 to 10.4 MeV, then to 30.5 MeV, and 50.0 MeV, respectively. The tanks are subdivided into a total of 10 sections with lengths varying between 3.16 m and 3.54 m (average 3.29 m) and dictated by positions of rf feed-loops (at L/4 and 3L/4 in the long tanks) and gaps. Copper-clad steel (15 mm steel + 2 mm copper) was used for the fabrication, with welded inserts to extend the copper to the circular joints between tank sections and to the rectangular girder slot. The departure from circular section introduced by this slot produces a resonant frequency decrease (300 kHz) which is less than the support stem frequency perturbation (in Tanks II and III) ; normally the bulk tuners introduce as much frequency perturbation. For fabrication simplicity the smaller holes were left unlined thus slightly increasing the rf losses. To assess the copper surface quality and the circular aluminium joints, rf measurements were made on Tank I without drift tubes, giving ∿ 80% of theoretical Q.

Drift Tubes. The cylindrical part of the drift tube body is an alignment reference surface, so one ensures accurate concentricity of the quadrupole magnetic axis by a close fit of the quadrupole yoke in the drift tube. It is closed by electron beam welding of the end cap(s) to the body and to the stainless steel bore tube. Water cooling is made via the stainless steel inner support stem which fits closely in the drift tube body. In addition to the standard dimensional checks on assembly, the flatness of the Tank I drift tube front faces and the shape of the Tanks II and III radiused profiles were checked by precise and quick capacitive methods.

Rf Feed Loops (Fig. 9). Two important criteria in the design were (a) large and predictable coupling variation with minimum movement and (b) minimum field perturbation. This leads to an eccentric line (outer diameter = 127 mm) near the cavity (which reduces coupling due to cavity field penetration), then a step up to the 230 mm coaxial line in which the PTFE ("Teflon") rf to vacuum window is mounted at about λ/2 from the short circuit at the cavity. The five loops installed perform reliably and give the specified coupling variation β = 1 to β = 4, for a movement of 30 mm.

Bulk Tuner (Fig. 3). This fixed tuner corrects the gross errors in frequency and field distribution so that in particular the final cavity resonant frequency falls in the piston tuner range. It is made in "T" sections ∿ 1 m long with the top of the "T" demountable so one can selectively

place the sections to make the first-order field and frequency corrections.

Piston Tuners. Of ten tuners mounted (one per structure section) only two per tank are used for automatic tuning as less than ± 5 kHz range is necessary at the correct cooling water temperature (20 °C) compared with ± 30 kHz available. A gap ∿ 1 mm was left between the tuner and the cavity wall in preference to installing a possibly unreliable sliding RF contact.

Post Couplers. To stabilize the field one post coupler is mounted per two drift tubes in Tanks I and II and one per drift tube in Tank III. The fields were set up by perturbation measurements[13] first by using variable penetration aluminum couplers, and then the final copper post couplers to produce greatly improved field stability in all tanks. For Tank I, where the accelerating field increases linearly with distance, the post penetration can be varied (in situ) by ± 5 mm and the orientation by ± 5°. In the other tanks the couplers are made to the fixed lengths predicted by the variable aluminium ones.

Rf Monitoring Loops. There are 34 pyrex thimbles mounted along the structure, allowing access to the H_ϕ field. Half of the available locations have unshielded matched loops (∿ 15 mm^2) which are adjusted by rotation to give a signal 40 dB relative to the tank input power. This is ample for all monitoring, frequency, rf level and phase control purposes.

Operational Reliability. There have been no failures on the structure which have required significant time for repairs since it came into service. A recent check has shown that there has been no decrease in cavity Q factors since installation.

High Energy Beam Transport (HEBT)

The 50-MeV beam line joins the old linac to the booster line at the bending magnet BH3 (see Fig. 4). This layout allows injection of the new linac beam either directly into the PS or into the booster. In the latter (normal) case one can use the old emittance line to check the matching of the beam to the booster, and the spectrometer line to adjust the three debuncher cavities for the required energy spectrum.

Focusing, Steering and Debunching. In the first part of the HEBT (before BH2), there is ample focusing (8 quadrupoles) to prepare the beam for the more critical achromatic part between (and including) bending magnets BH2 and BH3 (6 quadrupoles). Initially the beam is measured at the output of the Linac in the three phase planes which gives sufficient data for input to TRANSPORT. This program which can be run interactively with the CDC computers, gives results for quadrupole settings which can be used unmodified up to BH3 and thereafter the matching is made empirically by observation in the old single pulse emittance system and adjustment of 6 DC quadrupoles.

The beam steering is also critical, with 5 pulsed steering magnets adjusted systematically by reference to 8 magnetic beam position pickups to ensure > 95% transmission.

Ideally the first debuncher, DB11, adjusts the bunch length for best conditions at DB13 and DB14 (405.12 MHz) but one can often satisfy booster energy spread requirements with one (202.56 MHz) debuncher. However, for a recently-studied hollow distribution, DB14 is essential (see below).

Phase Plane Measurements[12]. With the two new measurement lines at the linac output, one can treat (one measurement per second) the horizontal and vertical planes and the longitudinal plane respectively. The data from the battery of collectors are treated and displayed similarly in all planes except for the units (mm, mrad) transversally, and (degrees, keV) longitudinally.

The Control System Design Features[5,31]

The control system is based on two DEC PDP 11/45 computers, each having 128k of core memory, in a back-up scheme. The control room consoles are all interfaced to seven CAMAC crates on a parallel branch. Each computer has access over a "branch mixer" to each crate and to a common Data Base of 64k of core memory, which contains status and description of each parameter and which interfaces to a special CAMAC module. Two 2.5 MHz serial CAMAC loops are also driven from the parallel CAMAC. One loop crosses the high voltage of the preinjector via infrared optical links to control the ion source parameters at 750 kV. The other loop links 14 CAMAC crates in the equipment gallery.

The system solves the mapping between a parameter name list to the CAMAC addresses, and may perform several CAMAC operations to achieve the desired result. All CAMAC activity related to process parameters is synchronized to the linac cycle (500 ms minimum). All system software, and some critical programs, are, for maximum speed, in MACRO-11 assembler language.

There are 900 individual parameters in the system, and about 1700 status bits for the surveillance task to handle. When a change in status or a parameter out-of-limits is detected, an alarm message gives the name of the process synoptic on which a flashing arrow indicates the offending parameter.

Due to the proximity of the preinjector, breakdown of the EHT occasionally blocks the computer. Normally the linac continues to function due to the local buffering of all command values. However, it is planned to install a "watch-dog" which will automatically reboot the computer if a blockage occurs. The MTBF of the computers was around 1200 hrs last year and still improving. The 384 CAMAC modules have a MTBF of 370 hrs. Serial CAMAC for the process has proven successful, with easier debugging than on the parallel CAMAC.

User acceptance of the control system has been very positive and several outside laboratories have shown interest in installing similar systems.

Rf System[11]

An independent rf chain fed from a common phase stable reference line is associated with each of the three bunchers, three tanks and four debunchers. Each chain comprises fast amplitude and

phase servo-mechanisms acting at low level, and a slow-cavity tuning servo. The control elements for phase (hybrids with varicaps) and for amplitude (PIN-diode attenuators) act on the low-level side of each chain; their structure is therefore the same throughout the whole rf system, with varying output of standard power amplifiers:

- 2 buncher chains with 35 kW available rf power
- 3 debuncher chains (110 kW available)
- 3 linac cavity chains with a total of 5 output amplifiers of 2.5 MW (2.2 MW required for 150 mA beam).

  Simple and reliable PFN-circuits together with a highly efficient charging circuit based on low-loss current-limiting chokes provide the 40 kV pulsed plate supply; FTH 170 triodes, a water-cooled version of the former FTH 470 are used in the final and drive stages.
- 2 second-harmonic stages of 25 kW each at 405.12 MHz feed the harmonic buncher and debuncher(DB14).

For a bunched beam in cavities operated near to zero crossing ($\cos\phi=0$), the phase and level control have to cope with a large reactive load as well as resistive loads from the cavity and varying in-phase beam components (e.g. in the third buncher and debunchers).

Performance

As already reported[8], the new CERN linac has met, practically from start, all the specifications including the maximum ouput current of 150 mA. Usually, running conditions are set according to demands from the first downstream accelerator (booster); the present operational beam characteristics are given in the following table:

Table 5 - Beam Characteristics

Symbol	Description, Units	Value
I	Intensity [mA]	125
E_{in}	750 keV emit. { $5E_{rms}$ / 90% of I } [π mm mrad]	40 / 50
E_{out}	50 MeV emit., 90% of I [π mm mrad]	15
$E_{\ell\ out}$	50 MeV long. emit., 90% of I, [π MeV degree]	7
W	Energy spread at "old meas. lines" [keV]	on request
$\frac{\Delta I}{I}$	Beam intensity ripple at 50 MeV [%]	±4

The transverse output emittance is considerably smaller than the specified one (25π mm mrad for 100 mA), in spite of an emittance increase factor in the linac of ≈ 2.5 (see Fig. 10). No specification was given for the longitudinal emittance, hence operating conditions are optimized for other parameters, leaving E_ℓ to increase in the linac by a factor ~ 5. On the contrary, precise requests concerning ΔW are given for the booster and the new debunching system can form a variety of energy distributions. Apart from "normal" distributions (see Fig. 11a), "hollow" distributions can be achieved by special combinations of the 3 debuncher settings[32] (see Fig. 11b).

Operation

The operation of the new CERN linac is considerably simplified by the possibilities offered on the control system. Essentially, one distinguishes between starting up and running the machine.

Start-up. The starting-up procedure is as follows:

1) Automatic formation of HT[15].
2) Setting of "groups" of parameters to reference values stored on disk; at present, touch buttons are allocated to ion source, LEBT,linac and HEBT focusing, rf (amplitudes and phases) LEBT steering and HEBT steering, respectively.
3) Control of beam intensities along the accelerator and emittance measurements at 50 MeV.
4) Log of all machine parameters.

Running. No permanent operator is needed in the linac control room. At present, the state of the machine is quickly obtained via process synoptics e.g. Fig. 7. In future, a "watch-dog" program should ease the control even more by indicating parameters which go out of the specified range.

Reliability

The reliability of all systems has been good. For the first two complete runs (each > 1000 hours) the downtime was 1.1% and 0.9%. A large fraction of this can be attributed to the inexperience of the operators and to a few "teething problems".

Acknowledgements

This project has actively involved the whole linac group with essential support in the PS Division, in particular on mechanical design, vacuum technology, magnetic measurements and mechanical and electronic fabrication. Additional help was provided within CERN on surveying and generally by SB Division. We have also profited from the traditional friendly collaboration with other labs and from the presence of many short and long term visitors. All the above have contributed significantly to the success of the project.

References

1. D. Warner (Editor), Project Study for a New 50 MeV Linear Accelerator for the CPS, CERN/MPS/LINP 73-1.
2. E. Boltezar, H. Haseroth, W. Pirkl, G. Plass, T.R. Sherwood, P. Standley, P. Têtu, U. Tallgren, D. Warner, M. Weiss, Review and Status of the CERN New 50 MeV Linac Project, Proc. of the 1976 Proton Linear Acc. Conf., p. 45, AECL-5677 (1976).
3. D. Warner, Accelerating Structure of the CERN New 50 MeV Linac, Ibid., p. 49.
4. D. Warner and M. Weiss, Beam Optics in the CERN 50 MeV Linac, Ibid, p. 245.
5. A. Cheretakis, J. Knott, P. Mead, A. van der Schueren and U. Tallgren, The Control System of the CERN New Linac, Ibd., p. 49.
6. J. Knott, D. Warner and M. Weiss, Adjustment of a Double Drift Harmonic Buncher and Bunch Shape Measurements, Ibid., p. 208.

7. J. Guyard and M. Weiss, Use of Beam Emittance Measurements in Matching Problems, Ibid., p. 254.
8. E. Boltezar, H. Haseroth, W. Pirkl, G. Plass, T. Sherwood, U. Tallgren, P. Têtu, D. Warner and M. Weiss, Performance of the New CERN 50 MeV Linac, Proc. of the 1979 Acc.Conf., IEEE Trans NS-26, No. 3 (1979), p. 3674.
9. E. Boltezar, Mechanical Design of the CERN Linac Accelerating Structure, This Conference.
10. H. Haseroth, M. Hone and J. Vallet, The Compensation for Beam Loading of the New CERN 50 MeV Linac, This Conference.
11. J. Cuperus, F. James and W. Pirkl, The RF system of the CERN "New Linac", This Conference.
12. P. Têtu, New Linac Three Phase Planes Pulsed Emittance Measurement, This Conference.
13. D. Warner, Calibration During Installation and During Initial Operation of the CERN 50 MeV Linac, This Conference.
14. M. Weiss, The Significance of Beam Optics Concepts as Applied to the New CERN Linac, This Conference.
15. H. Haseroth, Computer Controlled Formation of the 750 KeV Accelerating Column on the New CERN 50 MeV Linac, This Conference.
16. J. Grando, H. Haseroth, C. Hill and M. Hone, Tests with a Multi-Dipole Source on the CERN 500 keV Experimental Pre-accelerator, This Conference.
17. H. Haseroth and P. Têtu, Recent Operation and Modifications on the CPS 50 MeV Linac (Old Linac), Proc. 1976 Proton Linear Acc. Conf., p. 381, AECL-5677 (1976).
18. M. Weiss, Parameters of a New Linac Matched to Top PSB Performance, CERN/MPS/LINP/Note 72-1 (1972).
19. E. Boltezar, H. Malthouse and D. Warner, A 3 MeV Experimental Proton Linac, Proc. 1968 Proton Linac Acc. Conf., p. 626, BNL 50120 (1968).
20. D. Warner, Accelerator Research and Development with the CERN 3 MeV Linac, Proc. 1972 Proton Linear Acc. Conf., p. 33, LA-5115 (1972).
21. B. Bru and M. Weiss, Linac Quadrupole Gradients and Matching Parameters at Different Beam Intensities, Proc. 1970 Proton Linear Acc. Conf., p. 851, NAL (1970).
22. B. Bru and M. Weiss, Single and Double Drift Bunchers as Possible Injection Schemes for the CPS Linac. Proc. 1973 Particle Acc. Conf., IEEE Trans. Nucl. Sci., NS-29, p. 963 (1973).
23. R. Damm. A. Otis and V. Lo Grosso, Quadrupole Focusing System for the 200 MeV Linac, Proc. of the 1970 Proton Linear Acc. Conf., p. 561, NAL (1970).
24. R. Littlewood and C. Mazeline, The New Linac Quadrupole Measurement System, CERN/PS/SM/Note 78-8 (1978).
25. M. Bourgeois, Etude d'une Alimentation Pulsée et Régulée en Courant, CERN/MPS/LIN/Note 74-17 (1974).
26. M. Martini and D. Warner, Numerical Calculations of Linear Acc. Cavities, CERN 68-11(1968).
27. B. Bru and M. Weiss, Design of the Low Energy Beam Transport System for the New 50 MeV Linac, CERN/MPS/LIN 74-1 (1974).
28. P. Mead and U. Tallgren, Interfacing BASIC to the New Linac Control System, CERN/PS/LIN/Note 78-21 (1978).
29. B. Vosicki, M. Buzic and A. Cheretakis, The Duo-plasmatron Source for the CERN PS Linac, Proc. 1966 Linear Acc. Conf., p. 344, LA-3609 (1966).
30. J. Huguenin, R. Dubois, G. Visconti and R. El Bez, The New 500 keV Single Gap Preinjector Tube for the CERN Proton Synchrotron, Ibid., p. 355.
31. P. Mead, The System Software of the New Linac Control System, Proc. of the Digital Equipment Users Society, p. 93, Vol. 4, No. 1 (1977).
32. K. Schindl, Private Communication.

DISCUSSION

D.J. Liska, LASL: What was your reason for using aluminum seals throughout the machine?

Warner: They are cheap; the cavities do not need baking out and the force to deform them is small. Copper needs more (factor of 5) sealing force.

K. Mittag, Karlsruhe: How do the actual quadrupole settings used now correspond to those at the design stage - are they the same or did you change them?

Warner: We set them initially to $\mu = 30^{o}$ throughout the linac at one stage, but now μ is set slightly lower. As I pointed out, if we have an emittance growth, the μ will go up as you go along the linac because the space charge effect is decreasing. But we calculate quadrupole gradients with a program which has no emittance growth in it (normally).

K. Mittag: If you had used permanent quadrupoles to begin with, would the machine performance be as good now as it is?

Warner: We made a special attempt to bridge across the place where quadrupole sizes change and I am not sure you can do this with permanent magnet quadrupoles. I do not know whether you can design a permanent quadruple system to cover a large range of accelerated currents. In face, we lower the gradients for working at 50 mA or with a pencil beam. Even if permanent quadrupoles would have been available, I believe we still would have chosen quadrupoles which could be varied over the complete gradient range.

C. Curtis, FNAL: Starting with your design settings for the quads, have you then tried empirically various settings of the quads for the same beam current to see what happened to the quality of the beam?

Warner: We have the facility of adjusting the end quadrupoles (up or down) and the rest of the quadrupoles follow accordingly. This program is in FORTRAN. Now,the results are not very clear; there is a very broad optimum. I can give you an example. Where we varied the Tank II and III quadrupoles from 50% to 125% of normal operating level and

looked at the output beam position, it moved around, but the current only started to fall at about 60% of the normal operating level. So, you certainly could not use the beam current as a criterian for setting the quadrupoles.

Curtis: Did you measure the emittances at that time?

Warner: The emittances looked all right over a wide range, but this particular experiment was not aimed at measuring beam quality. We have not really investigated the beam quality as a function of the quadrupole law.

D. Hagerman, LASL: At LAMPF it has been essential to have the ability to reduce the quadrupole strength systematically so we can see what is going on inside a tank. It is a very tedious procedure, but I do not think we could have managed that machine without that technique being available. Therefore permanent quadrupole magnets would have been a bad choice.

S. Ohnuma, FNAL: Is the observed transverse emittance growth of 2 to 2.5 in agreement with the rms-type numerical calculation and, if so, what is the main cause of the emittance growth?

Warner: Our design predictions gave less transverse emittance growth but we made all our calculations with a larger input emittance (80π mm-mrad) compared to measured values of 50π-mm mrad. I believe we may have much less than that instantaneously because we measure the integrated emittance over 10 μsec. The longitudinal growth is also much higher than we calculate. To satisfy the booster synchrotron we are more concerned with the transverse emittance, but it is well within the acceptable level as we inject a much smaller emittance than was intended.

S. Ohnuma: Do you think you have gained a lot by having a fancy beam shaping system in the longitudinal phase space?

Warner: Yes. We insisted in the paper on the figure of merit being over 80% trapping, but the original aim was also to have the beam matched in longitudinal phase space at injection into the linac and we believe we have this also. We have not yet had much time for measurements but we will be able to do some more measurements in 1980.

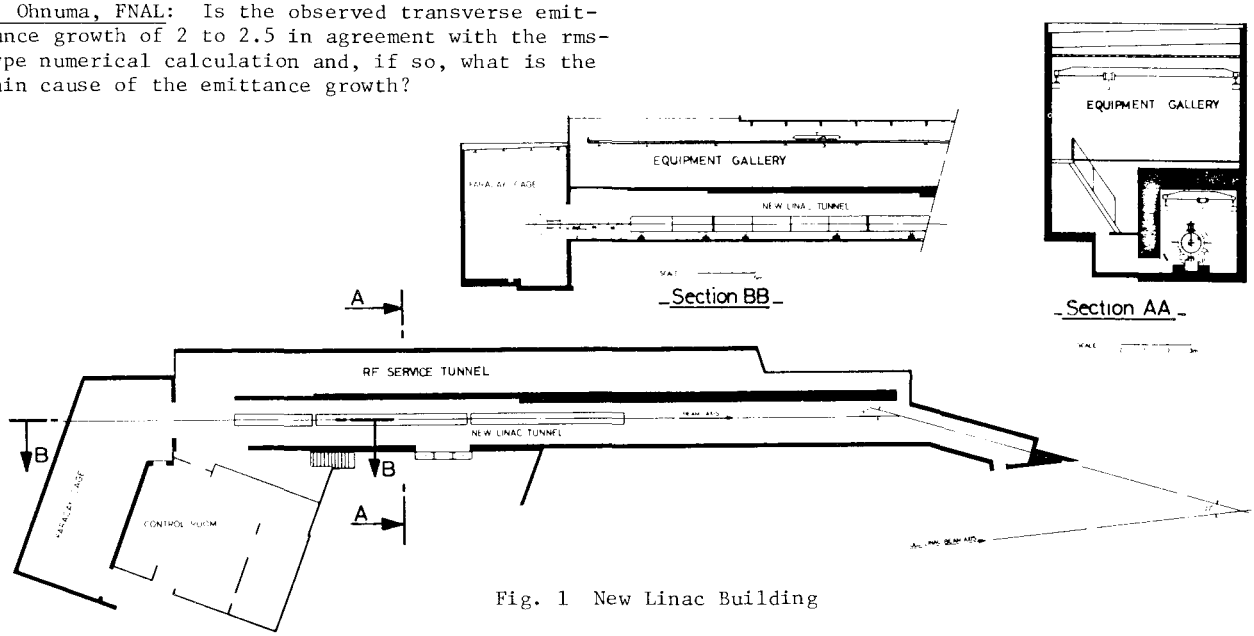

Fig. 1 New Linac Building

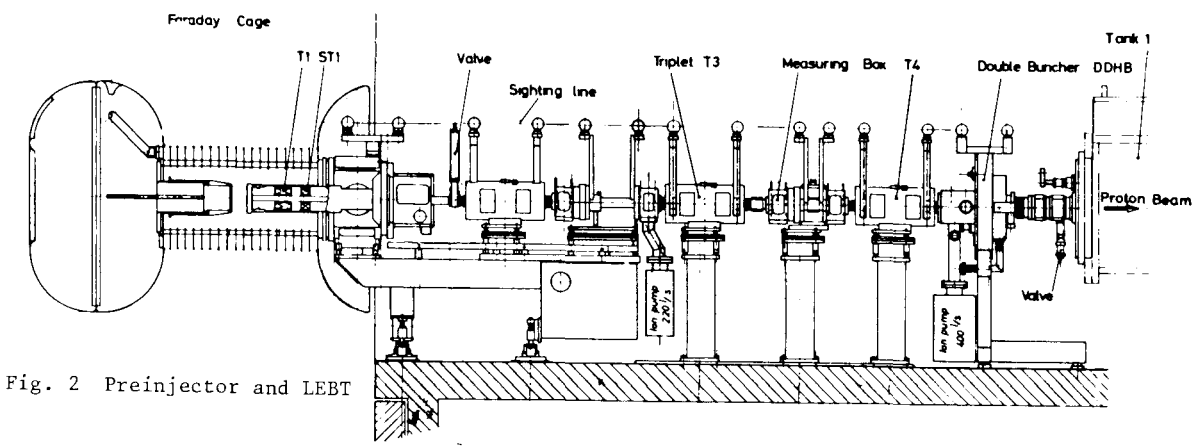

Fig. 2 Preinjector and LEBT

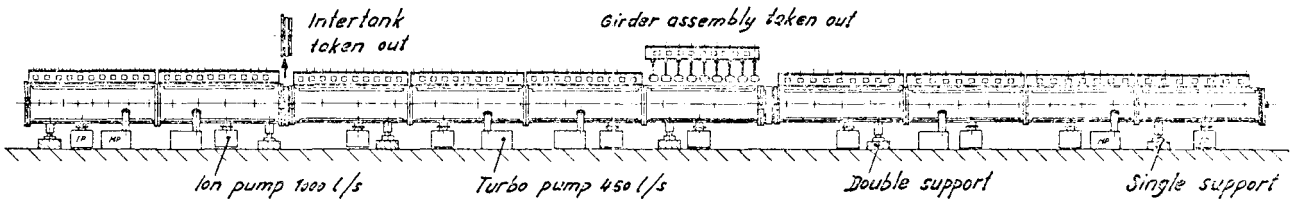

Fig. 3 Accelerating structure side view and cross-section above

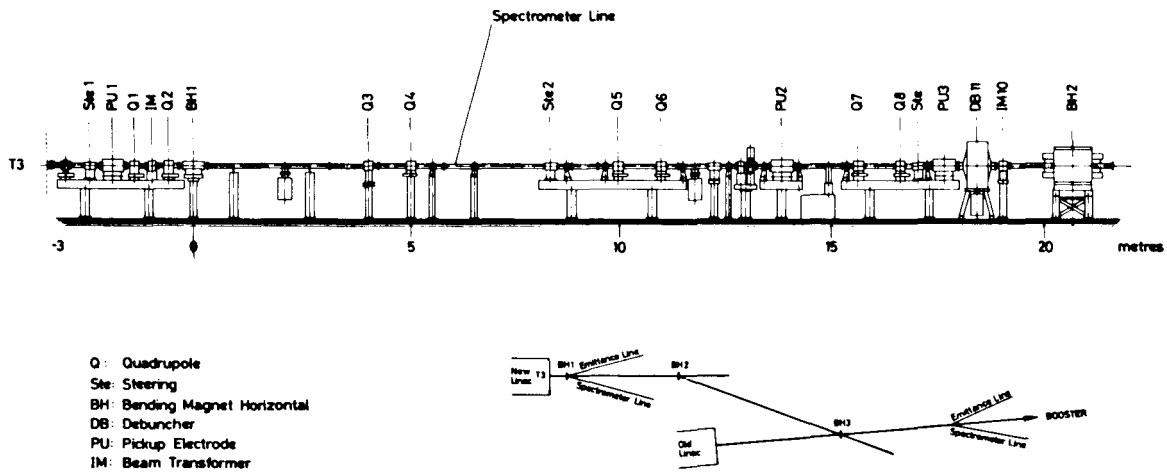

Fig. 4 HEBT side view to BH2 and schematic plan

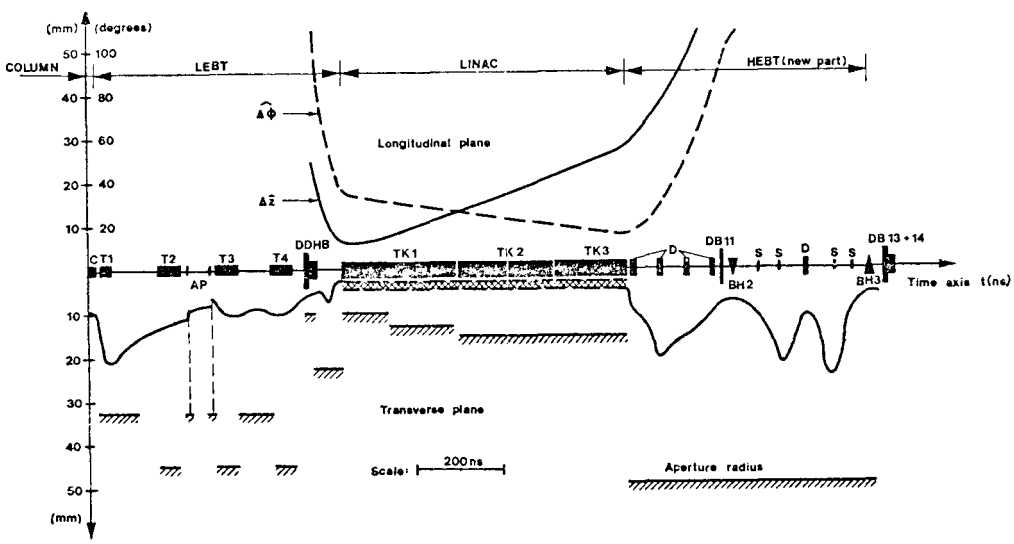

Fig. 5 Evolution of the beam from preinjector to debunchers

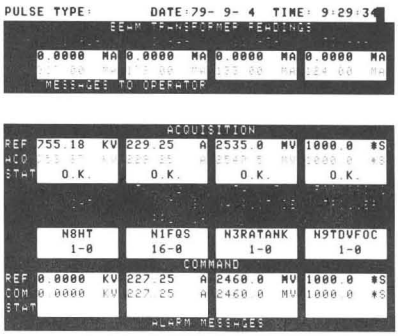

Fig. 6 Colour TV monitor on midiconsole

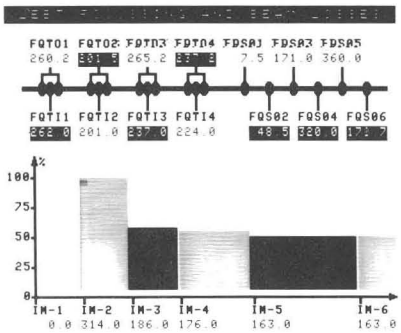

Fig. 7 Synoptic display of LEBT

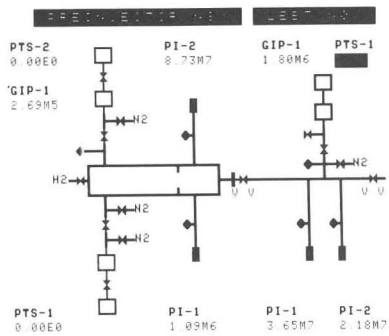

Fig. 8 Synoptic display of pre-injector and LEBT vacuum

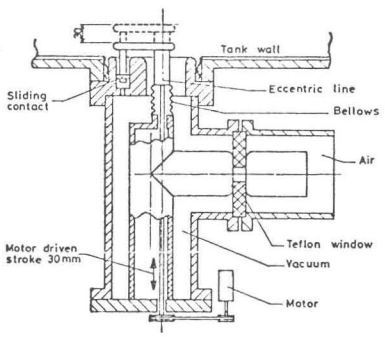

Fig. 9 RF Feed Loop (schematic)

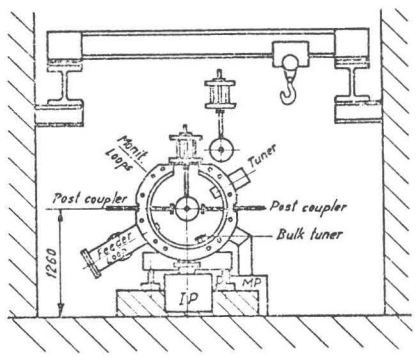

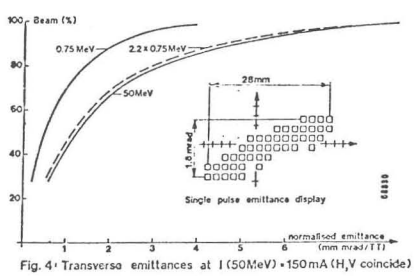

Fig. 4 Transverse emittances at I (50MeV) = 150 mA (H,V coincide)

Fig. 10 Transverse emittances for I = 150 mA (H,V coincide)

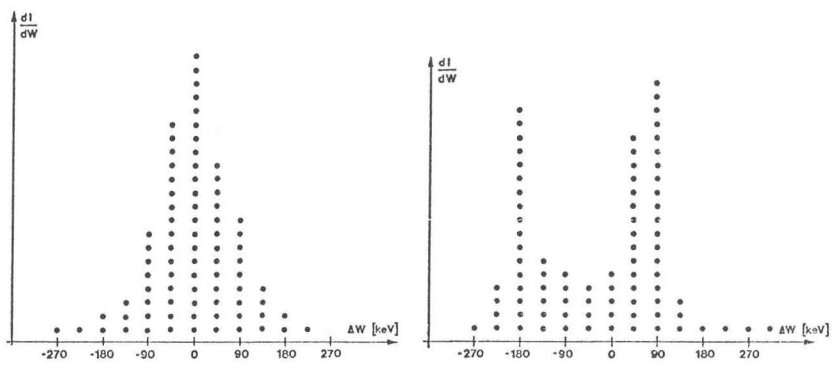

Fig. 11 Energy spectrum at "old" measuring lines
a) normal b) hollow